2021 43rd Annual International Conference of the
IEEE Engineering in Medicine & Biology Society (EMBC)
Oct 31 - Nov 4, 2021. Virtual Conference

Distinct Functional and Metabolic Alterations of DMN Subsystems in Alzheimer's Disease: A Simultaneous FDG-PET/fMRI Study

Ziyun Guan, Miao Zhang, Yaoyu Zhang, Biao Li, and Yao Li*, *Senior Member, IEEE*

***Abstract*—The default mode network (DMN) dysfunction has been widely identified in Alzheimer's disease (AD). Increasing evidence has shown that the functional heterogeneity of DMN has been associated with distinct cognitive functions. The pathophysiological changes of these two DMN subsystems, i.e., anterior DMN (aDMN) and posterior DMN (pDMN), also showed different patterns in the AD patients. Yet the underlying metabolic mechanism remains not clear. In this work, we performed a simultaneous FDG-PET/fMRI study, to investigate the distinct functional and metabolic alterations of DMN subsystems in AD. Significantly decreased functional connectivity strength (FCS) in pDMN but not aDMN was found in AD patients. The retaining connectivity in aDMN might represent a compensatory strategy. Concurrently, significant glucose hypometabolism was shown in pDMN and aDMN of AD patients, respectively. Moreover, the reduction of FCS in pDMN was positively correlated with MMSE score of patients. Our study suggests that resting state functional connectivity and glucose metabolism changed differently in the aDMN and pDMN of AD. Our findings brought new insights in understanding the underlying metabolism changes along with functional alterations in AD.**

I. Introduction

The default mode network (DMN) is the first large-scale system identified to be affected in AD [1]. In addition to its decreased functional connectivity (FC), a striking topographical resemblance of DMN was also described in other AD-related pathological findings, including amyloid deposition, atrophy and hypometabolism [2]. Increasing evidence has shown that the functional heterogeneity of DMN has been associated with distinct cognitive functions. For example, the anterior DMN (aDMN) has been involved in self-referential judgments, whereas the posterior DMN (pDMN) was mostly associated with successful recollection of prior experiences [3]. In previous AD studies, the pathophysiological changes of these two DMN subsystems also showed different patterns in the patients.

Using blood oxygen level-dependent (BOLD) functional magnetic resonance imaging (fMRI) technology, Myers et al. reported reduced FC in the pDMN of prodromal AD patients, but not in the aDMN [4]. Using ^{18}F-2-fluoro-2-deoxy-D-glucose positron emission tomography (FDG-PET) imaging, Fouquet et al. found the greatest metabolic decrease was in the pDMN of all amnestic mild cognitive impairment (aMCI) patients and greater metabolic decrease in the aDMN of aMCI patients who converted to AD [5]. FDG-PET reflects glucose metabolism from neurons directly, whereas BOLD fMRI approximates the neural activity by the fluctuations of deoxyhemoglobin concentration in the blood. Previous studies illustrated that the most energy of neurons were used for synaptic signaling [6]. Thus, there might be a fundamental link between glucose metabolism and neuronal activity. The investigation of the relationship between brain metabolic and functional changes in AD has been carried out using combined fMRI and FDG-PET methodology. For example, Mutlu et al. explored the influence of specific and global connectivity on the glucose hypometabolism in the AD patients [7]. However, in most studies, the functional and metabolic imaging data were acquired in different scans, which could bring the fluctuations of functional or metabolic features due to different brain states or moods of the person. The recently developed hybrid PET/MRI scanner allows simultaneous acquisition of FDG-PET and fMRI data, which provides an opportunity to explore the relationships or differences between concomitant intrinsic functional and metabolic changes in AD.

In this study, we used simultaneous resting-state FDG-PET/fMRI data to investigate the alterations of DMN subsystems, i.e., aDMN and pDMN, in AD patients. We evaluated the functional connectivity using functional connectivity strength (FCS) from fMRI data. The glucose metabolism was measured using standardized uptake value ratio (SUVR) from FDG-PET data. Additionally, the relationship between FCS and SUVR and their associations with global cognitive function were investigated. Our study provides useful insights into the understanding about the concurrent changes of functional and metabolic signals in the DMN subsystems of AD using an integrated PET/fMRI imaging methodology.

II. Materials And Methods

A. Participants

Nineteen AD patients (mean age: 67.26 ± 8.51, range from 54 to 83) and 22 age- gender- and education-matched cognitively normal controls (NCs) (mean age: 65.64 ± 7.47, range from 52 to 83) were involved in this study. All AD patients were recruited from the Memory Clinic at Ruijin Hospital, Shanghai. The NCs were recruited through local advertisements. The global cognitive function of each participant was evaluated by Mini-Mental State Examination (MMSE). The AD patients met the core clinical criteria proposed by the National Institute on Aging-Alzheimer's

This research was supported by National Natural Science Foundation of China (No. 81871083); Shanghai Jiao Tong University Scientific and Technological Innovation Funds (2019QYA12); Key Program of Multidisciplinary Cross Research Foundation of Shanghai Jiao Tong University (YG2021ZD28).

Ziyun Guan, Yaoyu Zhang and Yao Li (Tel: +86-21-62932981; e-mail: yaoli@sjtu.edu.cn) are with School of Biomedical Engineering, Shanghai Jiao Tong University, Shanghai, 200030, P.R. China. Miao Zhang and Biao Li are with Department of Nuclear Medicine, Ruijin Hospital, Shanghai Jiao Tong University School of Medicine, Shanghai, 200030, P.R. China.

Association (NIA-AA) workgroup. Exclusion criteria included: (1) psychiatric or other neurological disease; (2) pregnancy or renal failure; (3) major systemic disease; (4) history of traumatic brain injury; (5) drug or alcohol addiction. The study was approved by the Institutional Review Board of Ruijin Hospital and in accordance with the ethical standards of the Helsinki declaration. Written informed consents were obtained from all participants or their designees.

TABLE I. DEMOGRAPHIC AND CLINICAL DATA

	NC (n = 22)	AD (n = 19)	P-value
Age (years)	65.64(7.47)	67.26(8.51)	0.518[a]
Gender (male/female)	10/12	6/13	0.364[b]
Education (years)	13.32(2.42)	11.95(3.21)	0.127[a]
MMSE	29.55(0.74)	21.37(4.74)	< 0.001[a]

Values are listed as mean (SD). a. Independent two-sample t-test b. Chi-square test
Abbreviations: NC, normal controls; AD, Alzheimer's Disease; MMSE, Mini Mental State Exam.

B. *Imaging data acquisition*

All imaging data were acquired on a 3T integrated Siemens Biograph mMR scanner (Siemens Healthcare, Erlangen, Germany). Participants were required to fast for at least 6 hours before receiving a bolus injection of ^{18}F-FDG (3.7 MBq/kg). Simultaneous PET/MR imaging was performed at 40 min after the injection. The ^{18}F-FDG PET images were acquired in sinogram mode for 15 min (127 slices) and then reconstructed using ordered subset expectation maximization algorithm (21 subsets, 4 iterations) and post-filtered with an isotropic 2 mm full width half maximum (FWHM) Gaussian kernel. The reconstructed PET image voxel size was 2.1 × 2.1 × 2.0 mm^3. Attenuation correction was performed based on the Dixon method with an additional model-based bone compartment. The T1-weighted MR images were obtained using the magnetization-prepared rapid acquisition gradient echo (MPRAGE) sequence: repetition time (TR) = 1900 ms; echo time (TE) = 2.44 ms; flip angle (FA) = 9º; field of view (FOV) = 256 × 256 mm^2; voxel size = 0.5 × 0.5 × 1.0 mm^3; number of slices = 192. Resting-state fMRI images were obtained using echo-planar imaging sequence: TR = 2000 ms; TE = 22 ms; FOV = 192 × 192 mm^2; voxel size = 3.0 × 3.0 × 3.75 mm^3; number of slices = 36; number of volumes = 350.

C. *Imaging data preprocessing*

The fMRI data were preprocessed using the Analysis of Functional Neuroimaging (AFNI, https://afni.nimh.nih.gov) software. The first 10 volumes were removed to reduce the effects of noise and artifacts. Slice timing and head motion corrections were performed. To control head motion effects, volumes were censored if their framewise displacements were more than 0.5 mm. For each subject, at least 287 volumes, which was 9 minutes and 34 seconds in length, were preserved for further analysis. Nonlinear spatial normalization to the Montreal Neurological Institute (MNI)-152 template was performed, with an isotropic spatial resolution of 3 mm. Six head motion parameters and their first derivatives, averaged signals from white matter and cerebral spinal fluid, as well as the global signal were regressed out. Bandpass filtering from 0.01 to 0.1 Hz and spatial smoothing was performed with a 6 mm FWHM Gaussian kernel.

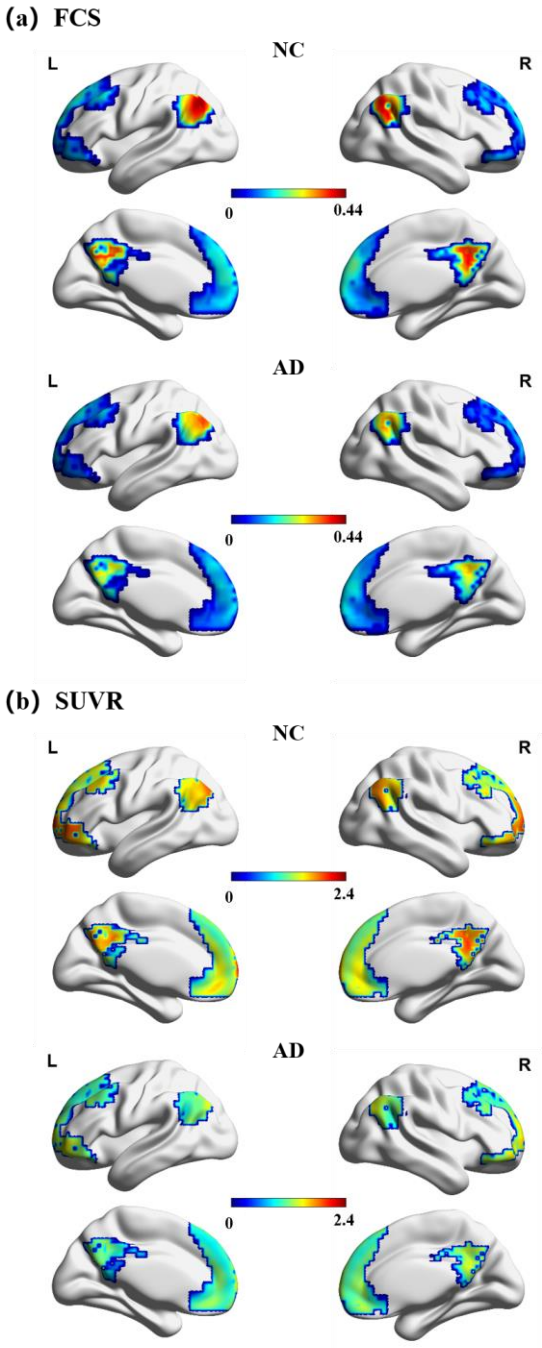

Figure 1. The FCS (a) and SUVR (b) maps in the whole DMN for NC and AD groups, respectively.

The preprocessing of FDG-PET data was carried out using SPM12 (https://www.fil.ion.ucl.ac.uk/spm). The FDG-PET data were first registered to the corresponding T1-weighted images using affine transformation and corrected for partial volume effects using the Müller-Gärtner method with toolbox PETPVE12. The T1-weighted images were spatially normalized to the MNI-152 template and the same transformation parameters were subsequently applied to warp the PET images to the standard MNI space. The PET data were quantified using the standardized uptake value ratio (SUVR), which was calculated as the ratio to the mean uptake of the

cerebellar gray matter. Finally, a 6 mm FWHM Gaussian kernel was applied for smoothing.

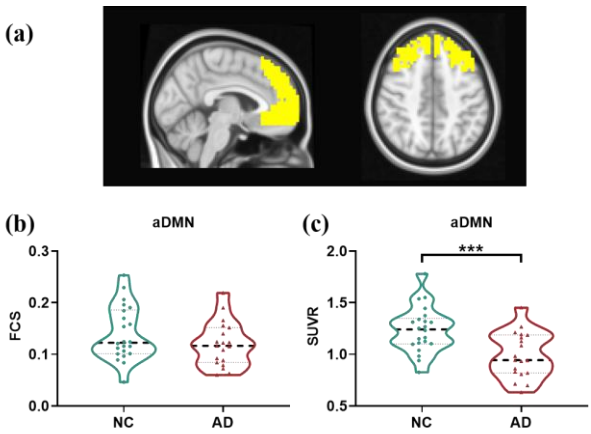

Figure 2. Group differences of FCS and SUVR in aDMN between AD patients and normal controls. (a) The mask of anterior default mode network. Differences of FCS (b) and SUVR (c) for aDMN between AD patients and normal controls. ***p < 0.001.

D. The parcellation of aDMN and pDMN

To obtain the DMN subnetworks, we first performed the whole-brain functional brain network parcellation on the NC group. The voxel-wise functional connectivity was evaluated using Pearson correlation coefficient calculated between the time courses of pair-wise voxels within the grey matter. To remove weak correlations that might arise from signal noises, a binary connectivity matrix was created with the data assigned to 1 if r > 0.2 and 0 otherwise. A sparse matrix was generated by group-averaging and discarding the connections present in less than half of the subjects. Finally, the infomap algorithm was used for parcellation of functional networks. The modularity Q was used to identify the optimal modular structure, which is defined as [8]:

$$Q = \frac{1}{L}\sum_{i,j\in N}[w_{ij} - \frac{k_i k_j}{L}]\delta_{m_i,m_j} \quad (1)$$

where i and j represent two individual nodes; L is the number of all edges in the network; $w_{i,j}$ denotes the connectivity strength between nodes i and j; k_i is the number of edges linked to node i and m_i denotes the module where node i belongs to. A network with a strong modular structure typically has a modularity Q ranged from 0.3 to 0.7. In our study, the calculated Q was equal to 0.61. The obtained aDMN was mainly composed of the medial prefrontal cortex and superior frontal gyrus, while the pDMN included posterior cingulate cortex, precuneus, and bilateral angular gyrus.

E. Intra-network FCS and SUVR analysis

The intra-network connectivity was evaluated by FCS. The FCS in each network was computed as the mean connectivity between a given voxel and all other voxels within the same network:

$$FCS = \frac{\sum_{i,j\in s} z_{i,j}}{N_s \times (N_s - 1)} \quad (2)$$

where N_s is the number of nodes within module s, and $z_{i,j}$ denotes the Fisher's z-transformed correlation coefficient r between voxel i an j within module s. The mean value of SUVR of voxels within the network was taken as the intra-network metabolism biomarker.

F. Statistical analysis

All the statistical analyses were carried out using SPSS software (version 25, IBM Corporation, Armonk, NY, USA). Normality tests were performed for all continuous variables using the Kolmogorov-Smirnov test. The demographics and clinical characteristics were compared between groups using independent two sample t-tests. In addition, Chi-square test was used for the gender comparison. General linear model (GLM) was used to compare the intra-network FCS and SUVR between NC and AD groups, with age, gender and education controlled. The relationship between functional connectivity and glucose metabolism as well as their relations with MMSE were explored using Pearson or Spearman partial correlation analyses depending on the normality of the data, with age, gender, and education as covariates.

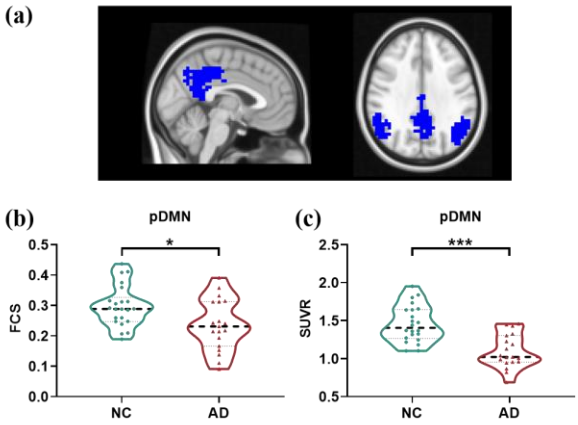

Figure 3. Group differences of FCS and SUVR in pDMN between AD patients and normal controls. (a) The mask of posterior default mode network. Differences of FCS (b) and SUVR (c) for pDMN between AD patients and normal controls. *p < 0.05, ***p < 0.001.

III. RESULTS

The demographic and clinical characteristics of the two groups are listed in Table I. No significant differences were found between patient and control groups in age, gender and education. The mean MMSE score of the AD group was 21.37 ± 4.74 (range from 9 to 27), which was significantly lower than the NC group (p < 0.001).

Figure 1 shows the distributions of FCS and SUVR in the whole DMN for NC and AD groups, respectively. The comparisons of mean FCS and mean SUVR for aDMN are shown in Figure 2, in which a significant reduction of SUVR was found in the AD group (p = 0.001) compared to the NC group. However, there was no difference in FCS between two groups in the aDMN. For pDMN, as shown in Figure 3, significant reductions of both FCS (p = 0.022) and SUVR (p < 0.001) were found in the AD group compared to the NC group. The coupling between functional connectivity and glucose metabolism was also investigated, but no significant correlations were found in either subsystem. The relationship between both measures and MMSE were also explored. For pDMN, the FCS was positively correlated with the MMSE

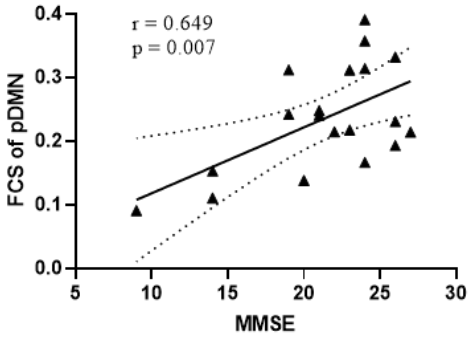

Figure 4. The FCS of pDMN was positively correlated with MMSE score in AD group. MMSE, Mini Mental State Exam.

score of AD patient ($p = 0.007$, $r = 0.649$), but the correlation between SUVR and MMSE was not significant ($p = 0.091$, $r = 0.437$). No correlations with MMSE for both FCS and SUVR were found in aDMN ($p > 0.5$) of AD patients.

IV. Discussion

Using simultaneous FDG-PET/rs-fMRI imaging, we characterized the patterns of functional connectivity and glucose metabolism in aDMN and pDMN of AD patients. In the pDMN, functional connectivity and glucose metabolism significantly reduced and the FCS of pDMN was positively correlated with global cognitive status in AD. In the aDMN, however, significantly reduced glucose metabolism, but not functional connectivity, were observed in AD patients compared to NCs.

Pathophysiological alterations in the pDMN regions of AD patients have been widely investigated. Previous studies have reported decreased functional connectivity and glucose metabolism in the medial and lateral parietal cortices [9]. Some studies found amyloid-β accumulation in pDMN coincided with hypometabolism in the same regions [10]. The amyloid-β accumulation was negatively correlated with intrinsic connectivity [4]. These findings indicate a close relationship between the compromised functional connectivity and pathological and metabolic changes in the pDMN of AD.

The aDMN neuronal dysfunction was thought to be related to late stage of AD [11]. A previous study has found the metabolic derangement in frontal region was later than that in posterior cingulate cortex [9]. In a longitudinal study of DMN subnetworks, an initially increased connectivity and a subsequently decreased connectivity were reported in the aDMN [12]. Jones et al. isolated four subsystems of DMN and found increased and decreased dynamic connectivity for anterior and posterior subsystems, respectively, in AD [13]. Our study found decreased glucose metabolism but unaffected connectivity in the aDMN of AD. The increasing or retaining connectivity in aDMN have typically been interpreted to represent a compensatory phenomenon to support better performance on cognitive tasks, or a shift of processing burden from pDMN and medial temporal lobe to downstream aDMN [14].

Finally, the impaired connectivity of pDMN showed significant correlations with global cognitive status in AD patients. This may be due to the fact that the pDMN was impaired earlier and more severe compared to the aDMN [13]. Besides, the PCC, hippocampus and angular gyrus have been typically associated with episodic memory retrieval, autobiographical memory and semantic memory related to internal thoughts [15]. Such memory conditions are considered as the hallmarks of AD. Together, pDMN dysfunction is a major and consistent feature in AD patients. We found a trend-wise correlation but the significance was not reached between hypometabolism of pDMN and global cognitive status, which might be limited by the amount of data.

In summary, our study suggested that resting state functional connectivity and glucose metabolism changed differently in the aDMN and pDMN of AD. Consistent reductions of connectivity and metabolism in pDMN were associated with clinical performance. Whereas the retaining connectivity in aDMN might represent a compensatory strategy. Our findings brought new insights in understanding the underlying metabolism changes along with functional alterations in AD.

References

[1] M. D. Greicius, G. Srivastava, A. L. Reiss, and V. Menon, "Default-mode network activity distinguishes Alzheimer's disease from healthy aging: evidence from functional MRI," Proc Natl Acad Sci U S A, vol. 101, no. 13, pp. 4637-42, 2004.

[2] R. L. Buckner et al., "Molecular, structural, and functional characterization of Alzheimer's disease: evidence for a relationship between default activity, amyloid, and memory," J Neurosci, vol. 25, no. 34, pp. 7709-17, 2005.

[3] M. E. Raichle, "The brain's default mode network," Annu Rev Neurosci, vol. 38, pp. 433-47, 2015.

[4] N. Myers et al., "Within-patient correspondence of amyloid-β and intrinsic network connectivity in Alzheimer's disease," Brain, vol. 137, no. Pt 7, pp. 2052-64, 2014.

[5] M. Fouquet et al., "Longitudinal brain metabolic changes from amnestic mild cognitive impairment to Alzheimer's disease," Brain, vol. 132, no. Pt 8, pp. 2058-67, 2009.

[6] O. Kann and R. Kovács, "Mitochondria and neuronal activity," Am J Physiol Cell Physiol, vol. 292, no. 2, pp. C641-57, 2007.

[7] J. Mutlu, B. Landeau, M. Gaubert, V. de La Sayette, B. Desgranges, and G. Chételat, "Distinct influence of specific versus global connectivity on the different Alzheimer's disease biomarkers," Brain, vol. 140, no. 12, pp. 3317-3328, 2017.

[8] M. Rosvall and C. T. Bergstrom, "Maps of random walks on complex networks reveal community structure," Proc Natl Acad Sci U S A, vol. 105, no. 4, pp. 1118-23, 2008.

[9] M. Scherr et al., "Decoupling of Local Metabolic Activity and Functional Connectivity Links to Amyloid in Alzheimer's Disease," J Alzheimers Dis, vol. 64, no. 2, pp. 405-415, 2018.

[10] M. J. Grothe and S. J. Teipel, "Spatial patterns of atrophy, hypometabolism, and amyloid deposition in Alzheimer's disease correspond to dissociable functional brain networks," Hum Brain Mapp, vol. 37, no. 1, pp. 35-53, 2016.

[11] J. B. Langbaum et al., "Categorical and correlational analyses of baseline fluorodeoxyglucose positron emission tomography images from the Alzheimer's Disease Neuroimaging Initiative (ADNI)," Neuroimage, vol. 45, no. 4, pp. 1107-16, 2009.

[12] J. S. Damoiseaux, K. E. Prater, B. L. Miller, and M. D. Greicius, "Functional connectivity tracks clinical deterioration in Alzheimer's disease," Neurobiol Aging, vol. 33, no. 4, pp. 828.e19-30, 2012.

[13] D. T. Jones et al., "Cascading network failure across the Alzheimer's disease spectrum," Brain, vol. 139, no. Pt 2, pp. 547-62, 2016.

[14] E. C. Mormino et al., "Relationships between β-amyloid and functional connectivity in different components of the default mode network in aging," Cereb Cortex, vol. 21, no. 10, pp. 2399-407, 2011.

[15] V. Menon, "Large-scale brain networks and psychopathology: a unifying triple network model," Trends Cogn Sci, vol. 15, no. 10, pp. 483-506, 2011.